

**Paper n° IAF – 00 – Q.1.08**

**THE INTEGRAL OPTICAL MONITORING  
CAMERA DESIGN, QUALIFICATION TESTS AND  
LESSONS LEARNED**

J.M. Defise, E. Mazy, J.Y. Plesseria, E. Renotte, P. Rochus

Centre Spatial de Liège , Ave. du Pré-Aily,  
B4031 Liège,  
Belgium

**51<sup>st</sup> International Astronautical Congress  
2 – 6 Oct 2000 / Rio de Janeiro, Brazil**

# THE INTEGRAL OPTICAL MONITORING CAMERA DESIGN, QUALIFICATION TESTS AND LESSONS LEARNED

Jean-Marc Defise, Emmanuel Mazy, Jean-Yves Plessier, Etienne Renotte, Pierre Rochus  
Centre Spatial de Liège, Ave. du Pré-Aily,  
B4031 Liège,  
Belgium

## 1. ABSTRACT

The Optical Monitoring Camera (OMC) is part of the science payload developed for the ESA INTEGRAL mission, scheduled to be launched in 2002. The OMC is an imager that will monitor star variations in the V-band. This paper presents the design of 3 sub-systems of OMC: the optics, the baffle and the cover mechanism. It describes the acceptance tests performed at Centre Spatial de Liège (CSL) on the qualification model at sub-system level and at instrument level. The QM test results are discussed and the lessons learned are used to improve the FM elements.

The optical system is based on a 6-lens objective mounted in a titanium alloy barrel. Mechanical and thermal behaviours in space environment are verified in CSL premises. Specific tests have been developed to detect possible degradations resulting from environmental constraints.

The baffle consists in a 600 mm length aluminium alloy cylinder surrounding the optical system and the internal vanes. It has been designed to reach the very high level of straylight rejection required by the science goals of the instrument.

The cover system is basically a door mechanism and a sunshade. The door is closed during integration and launch to prevent dust contamination of optics. The mechanism will be operated only once in flight but has to be intensively tested on ground to assess its very high reliability level.

The OMC qualification model was tested at camera unit level at a very late stage in the program for thermal and optical behaviour in space environment. Discrepancies were observed in the optical tests: unexpected sources of straylight decrease the optical quality of the system. Identification of straylight sources and improvement of the flight model design are discussed.

## 2. DESCRIPTION

### 1.1. INTEGRAL

The Optical Monitoring Camera (OMC) is a part of the INTEGRAL payload (figure 1), an ESA scientific mission (INTERNATIONAL Gamma-Ray Astrophysics Laboratory) dedicated to the fine spectroscopy and fine imaging of celestial gamma-ray sources. INTEGRAL covers the energy range from 15 keV to 10 MeV with

concurrent monitoring in the X-ray (3-35 keV) and optical (V-band) energy range. The spacecraft is scheduled to be launched in April 2002 with a PROTON although all environmental specifications had also to be fulfilled for the ARIANE 5 alternative option.

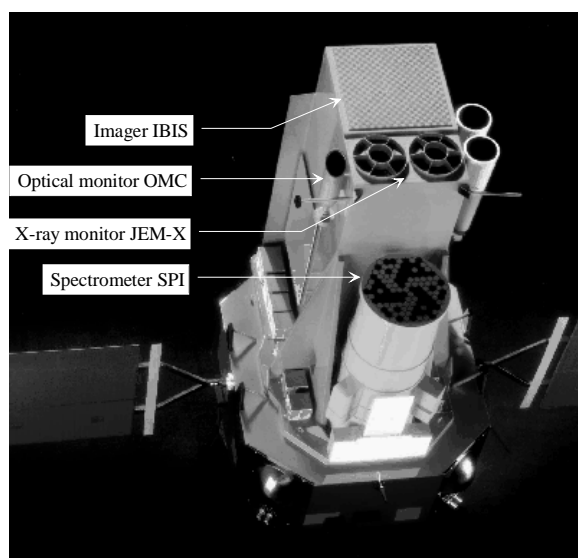


Figure 1: Integral payload

### 1.2. OMC

The OMC instrument (figure 2) consists of a CCD camera unit connected to a single dedicated electronic unit. It is a 20 kg class instrument mounted on the top of the INTEGRAL payload module. The camera unit is based on a large format CCD (2048x1024 pixels) working in frame transfer mode (1024x1024 pixel image area) that avoids the use of a mechanical shutter. The CCD is cooled by means of a passive radiator down to operational temperatures lower than -80°C for noise reduction purposes. An optical baffle affords the necessary reduction of straylight required for faint source detection up to  $m_v = 19.7$ . A one-shot deployable cover is used to protect the optics and the baffle interior from contamination during ground testing, launch and early days in orbit.

The main optical requirements of the instrument are listed in table 1. The FOV is defined by the payload pointing mode. It is a compromise between the source confusion and the FOV of other instruments on the

payload, particularly the X monitoring instruments. The V-band selection is achieved with a specific filter inserted in the optical system.

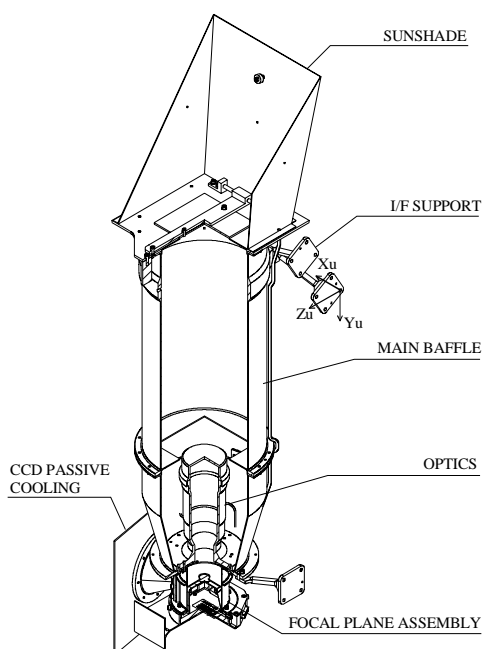


**Figure 2:** OMC instrument

Aperture size:	50 mm diameter
Field of View (FOV):	5 x 5 arcdeg square
Pixel size:	13 x 13 $\mu\text{m}^2$ (17.6 x 17.6 arcsec <sup>2</sup> )
Spectral range:	V-band centred at 550 nm
Sensitivity:	19.7 visual magnitude

**Table 1:** OMC specifications.

CSL is responsible for the design, fabrication and sub-system level verification of three elements: the main baffle, the optical system and the cover system. Those elements were integrated into the Camera Unit under INTA responsibility and tested at INTA and at CSL for environmental tests. Other main sub-systems are the focal plane assembly, the radiators, the thermal and electrical elements (electronic box, MLI, harnesses...). The qualification and acceptance campaign of the OMC is based on four models: the Structural and Thermal Model (STM), the Engineering Model (EM), the Qualification Model (QM) and the Flight Model

(FM). The qualification is performed on the STM, EM and QM. Nevertheless, as the QM will be used as Flight Spare Model (SFM), it is required that the QM sub-elements are not submitted to qualification levels.

### 1.3. Optical system

The parameters driving the design are summarised in table 2. The optical performances must be met within the operational conditions range while the non-operational environment defines the extreme conditions that shall be withstood without damage. The nominal operational temperature and the very wide temperature ranges result from the thermal design of the instrument. Moreover, the thermal requirements at the interfaces dictate the lens barrel material: titanium alloy.

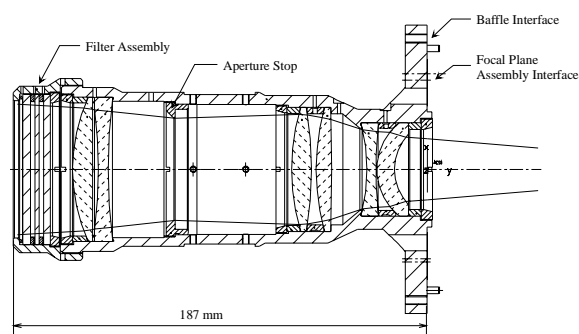


**Figure 3:** Cut-view of the optical system QM

The optical design (figure 3) is based on six radiation-hard lenses (F/3) housed in a titanium barrel [1]. A filter assembly holds two colored filters (Schott BG39 and GG495) defining the useful spectral range. An additional Schott BK7G18 glass plate protects the filters from direct radiation. The filters and the protective plates are maintained with a retainer and an O-ring.

The titanium material is coated with black chromium for straylight purposes. All optical surfaces are coated with anti-reflection coating (W-coat) for radiometry purposes, excepted the first optical surface, viewing the cold space, which is free of coating to avoid coating degradation under radiation.

Encircled energy:	> 70% in a pixel (13x13 $\mu\text{m}^2$ )
Modulation Transfer Function (MTF):	> 70% at Nyquist Frequency (38.5 c/mm)
Backfocus:	$\approx$ 50 mm
Transmission (@550 nm):	> 70% at the beginning of life (> 60% EOL)
Backfocus (part of Focal Plane assembly) material:	INVAR material
Radiation dose:	42 krad over 5 years in case of Ariane V launcher
Nominal conditions :	0°C (in vacuum)
Thermal range (operational conditions):	-20°C to +20°C
Thermal range (non-operational conditions):	-80°C to +45°C
Vibrations (non-operational conditions):	Random: 27 $\text{g}_{\text{RMS}}$ in the range 20 – 2000 Hz

**Table 2:** Optical requirements and environmental conditions.

#### 1.4. Main baffle

The main baffle was designed to achieve the high rejection factor required for observation of stars up to visual magnitude of 19.7. The design is described in [2] and figure 4 where its straylight performances were investigated. The main baffle consists of a cylinder and a cone, both made of aluminium. On these tubes, interfaces are added for the optical system, for the cover system, for the alignment cube, for the mounting legs, for the lifting tool, for the MLI grounding and for

the electrical connectors. Inside this tube, 4 square aperture vanes are inserted for straylight purpose. A venting hole is also included in the design to allow depressurization without parasitic light. All the internal surfaces are black anodised to damp all the reflections. The main baffle mechanical design was placed under INTA's responsibility as it is the main structural piece of the OMC instrument, which holds all other sub-systems. Baffling vanes and venting device were defined by CSL.

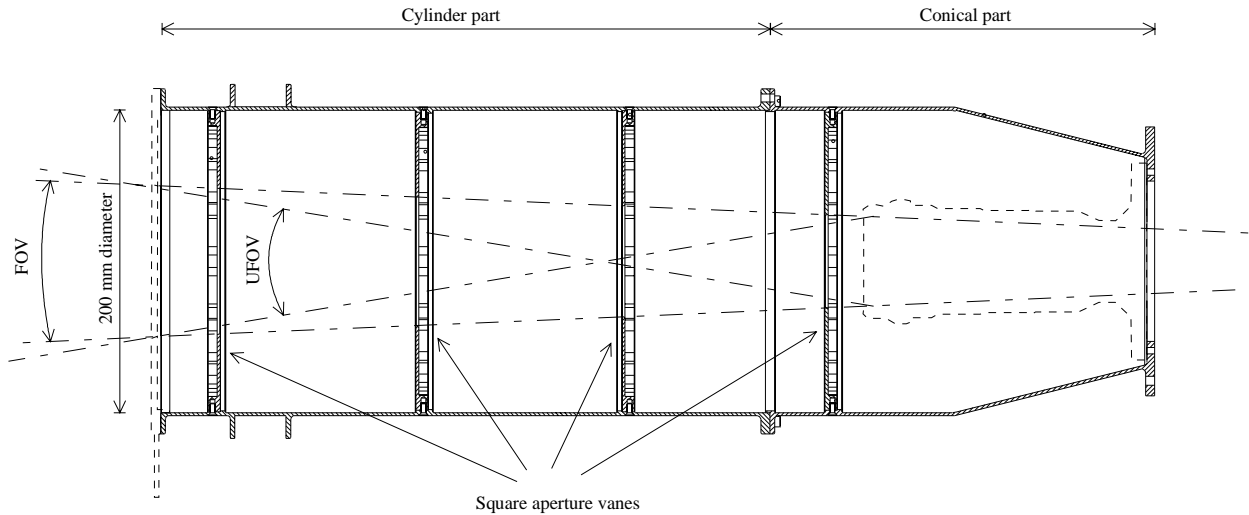


Figure 4: Cut view of the OMC main baffle.

#### 1.5. Cover system

The goal of the cover system is to prevent particles from entering the main baffle. It must be kept closed during integration and launch and opened only once in orbit. The cover system also includes a sunshade (figure 5) that protects the cover mechanism and the aperture of the main baffle from direct sunlight. The position of the sun is 50 arcdeg apart from the optical axis (worst case). The cover mechanism and the sunshade are mounted on an interface plate that is also the interface with the main baffle and the first vane of the baffling system. The sunshade consists in 3 aluminium walls, stiffened with U-section aluminium beams.

The mechanism is based on a paraffin actuator developed by Starsys Research Corporation. An internal mechanism maintains a T-shaped bar. This T-bar is mounted on a locking arm that maintains a cover lid on the aperture in the interface plate. The lid is spring-mounted to the arm to provide for intimate contact with the interface plate.

Two torsion springs, mounted around a stainless steel shaft, provide the opening torque. Once the T-bar is released by the paraffin actuator, the springs open the door and maintain it opened. A starlock washer is

used as a redundancy to maintain the door in open position. It is a washer with a star-shape aperture that can slide in only one direction on a rod. It is mounted on the locking arm and will be slipped on a clamping rod at the end of the opening.

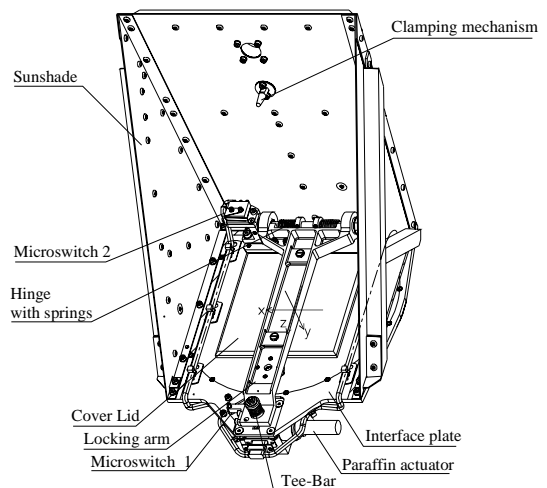


Figure 5: Cover system description.

Two microswitches are included in the design to verify the status of the door. One is located near the paraffin actuator (#1) to monitor the closed position,

the other one (#2) is located near the hinge to check the open position. The connection of the paraffin actuator and the microswitches to the OMC electronic unit is performed through a 9 socket sub-D connector located under the interface plate.

### 3. QM SUB-SYSTEMS TESTS

#### 3.1. Test philosophy

Prior to final assembly at instrument level, sub-systems were evaluated at CSL through performance and environmental tests. Functional tests are performed between each environmental test to verify possible degradations of performances. The table 3 summarises the test philosophy performed on all sub-system items [3].

	Optical system	Cover system	Main baffle
STM	Vib (Q)		
DM	Vib (Q)	Vib, TV Lifetime (Q)	
EM			
QM/ SFM	Funct Vib (A) TV (A)	Funct Vib(A) TV (A)	
FM	Funct Vib (A) TV (A)	Funct Vib (A) TV (A)	Stray- light

Funct: functional test Q: qualification level  
TV: thermal vacuum test A: acceptance level  
Vib: Vibration test

**Table 3:** Qualification and acceptance summary.

The environmental tests consist in a thermal vacuum test in order to verify that the specimen will survive to thermal cycling and in a vibration test in order to verify that the specimen will survive to launch loads without degradations.

#### 3.2. Optical system QM

The behaviour of the optical system QM against environmental conditions was tested at acceptance level after qualification on the DM. Between each environmental test, a wavefront error (WFE) measurement allowed verifying any misalignment or failure.

The levels applied in the vibration test are the acceptance levels defined in table 4 and 5 along 2 axes (axial and lateral). The measured eigenfrequencies were close to the ones observed on the STM (620 Hz lateral and 2200 Hz in axial direction), the difference being explained by the slight difference in mass between the two models.

Frequency (Hz)	Acceleration level
5- 21	± 7.33 mm
21 - 60	± 13.33 g
60 - 100	± 4 g

Sweep rate: 4 octaves/minute  
1 sweep up

**Table 4:** Sine vibration test levels.

Axis	Freq (Hz)	PSD level	Rms Acceleration
Lateral X	20 - 100 100 - 2000	+6 dB/octave 0.178 g <sup>2</sup> /Hz	18.402 grms
Axial Y	20 - 100 100 - 2000	+6 dB/octave 0.133 g <sup>2</sup> /Hz	15.937 grms

Duration of test: 1 minutes each axis

**Table 5:** Random vibration test levels.

Although no visible damage was detected, the optical verifications showed slight modifications in WFE due to stress release inducing micro-settings of lenses (table 6). Those small changes did not induce loss in performances since MTF measurements showed optical performances within specifications.

For the thermal vacuum test, the optical system was mounted on a regulated conductive interface and installed in FOCAL 1.5 vacuum chamber at CSL. Radiative thermal panels were surrounding the specimen. All panels were regulated in serial with one nitrogen gas line. Figure 6 shows the optical system QM equipped with its thermal sensors. The test consisted in one thermal cycle in the non-operational temperature range (+50°C, -45°C) and 3 cycles in the operational temperature range (+25°C, -25°C).

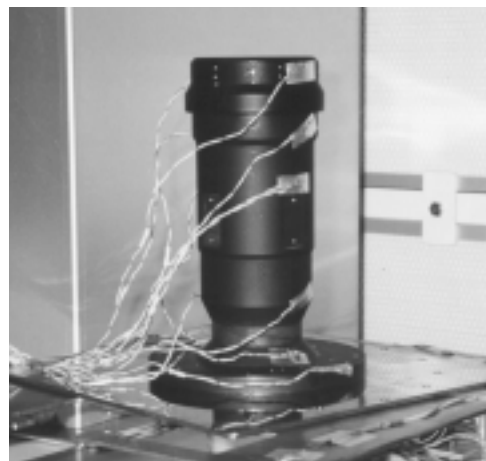


**Figure 6:** optical system instrumented with thermocouples.

The WFE measurement consists in an on-axis measurement of the optical system at 633 nm in vertical position to limit gravity effects. Table 6

shows the WFE test results. The variations in the WFE come from micro-settings of lenses but the MTF degradation is too small for measuring.

	WFE RMS [wave]	WFE P-V [wave]
Reference	0.078	0.797
Post vibration 1 test	0.162	0.917
Post vibration 2 test	0.115	0.774
Post thermal test	0.124	0.854

**Table 6:** WFE measurement results.

### 3.3. Cover system QM

The cover system QM was tested at CSL with an identical test plan: a vibration test followed by a thermal vacuum test. Functional tests after each environmental test allowed verifying possible degradations.

The goal of the functional tests is to verify that the cover will open within the required time (less than 300 seconds) after the different environmental condition exposures and during thermal vacuum test at high and low operational temperatures. The two circuits (nominal and redundant) will be verified. All activations were successful with a nominal current between 350 and 356 mA and with a release time ranging from 54 seconds (40°C in vacuum) to 180 seconds (-45°C in vacuum).

The cover system was shaken along its three reference axes with the levels described in table 7 and 8.

Frequency (Hz)	Acceleration level
5- 21	± 7.33 mm
21 - 60	± 13.33 g
60 - 100	± 4 g

Sweep rate: 4 octaves/minute  
1 sweep up

**Table 7:** Sine vibration test levels.

Axis	Freq (Hz)	PSD level	Rms Acc.
Lateral Z	20 - 100	+6 dB/octave	13.14 grms
	100 - 2000	0.089 g <sup>2</sup> /Hz	
Lateral X	20 - 100	+6 dB/octave	21.518 grms
	100 - 334	0.178 g <sup>2</sup> /Hz	
	334 - 440	+12 dB/octave	
	440 - 650	0.533 g <sup>2</sup> /Hz	
	650 - 856	-12 dB/octave	
856 - 2000	0.178 g <sup>2</sup> /Hz		
Axial Y	20 - 100	+6 dB/octave	16.09grms
	100 - 2000	0.133 g <sup>2</sup> /Hz	

Duration of test: 1 minutes each axis

**Table 8:** Random vibration test levels.

The required levels were applied without notching and the main structure survived the test. The eigenfrequencies observed were very similar to the ones observed during STM-DM campaign except for the locking arm that was slightly modified for the QM and FM.

Nevertheless, two discrepancies were observed after vibration test. One screw of the internal connector was found loosened. Most likely, it was not properly torqued. This has no impact on the connection. The second discrepancy was more important: the microswitch 1 (that verifies the closed position) was no longer activated. This was due to a bad positioning of the lever screw. No sufficient margin was taken and slight displacement of the locking arm lead to release the pressure on the microswitch. By correcting this problem, it was also pointed out that the microswitches mounting was not adequate and that it decreases the operating range of the microswitch lever. The two problems have been corrected for the FM.

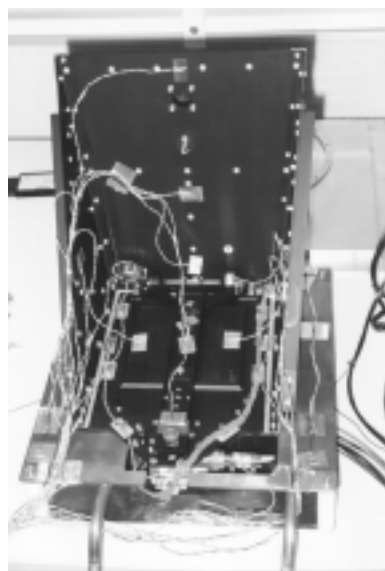


**Figure 7:** Cover system instrumented with thermocouples.

The goal of the thermal vacuum test is to verify that the cover system could operate at low and high operational temperature under vacuum and that it can survive to non-operational temperatures and cyclings. The setup was identical to the one of the optical system (figure 7). Four cycles were performed: a non-operational temperature cycle (+40°C, -95°C) followed by 3 operational temperature cycles (+40°C, -45°C). A first functional test was performed at the first hot case stabilisation (+40°C) followed by a pressure recovery for manual resetting of the mechanism. A second was performed at the first operational cold case stabilisation (-45°C) followed

also by a pressure recovery. The last functional test was performed at the end of the last operational cold case stabilisation (-45°C).

#### 4. CAMERA UNIT TEST

In February 2000, the complete camera unit QM was tested in the CSL FOCAL 3 vacuum chamber with a team of INTA. The test purpose was to verify the thermal behaviour in operational conditions (thermal balance) and to verify if the instrument can survive to thermal cyclings in operational and non-operational temperature range (thermal vacuum). Tests of electronics and cover system opening were performed to verify the complete functionality of the instrument. Moreover, optical tests allowed verifying the optical performances in nominal, cold and hot operational thermal conditions. CSL was responsible of the test facility, the thermal environment and the OGSE/MGSE.

##### 4.1. Test set-up

The vacuum test was performed in a 3 meters diameter vacuum chamber equipped with a vibration-free optical bench isolated from the ground and the chamber (figure 9). OMC QM was surrounded by 5 independent radiative thermal panels that define the thermal environment viewed by the instrument (figure 10). The bottom panel of the thermal box is substituted by multilayer insulation covered with a black Kapton top layer for straylight purpose. The 3 legs of the instrument were thermally controlled by means of heaters and copper plates linked to a small thermal panel (figure 8). All panels are thermally controlled with nitrogen gas. The OMC QM legs were interfaced on a goniometric support, which

allows field of view analysis up to  $\pm 10$  arcdeg with a 3.6 arcsec resolution scanning.

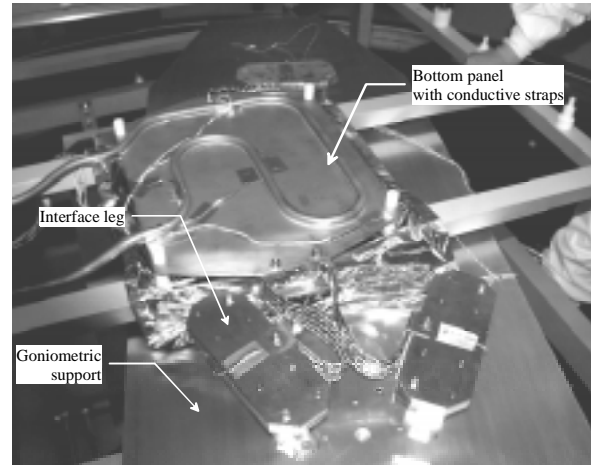


**Figure 8:** Interface legs with its bottom panel.

This support is mounted on the optical bench of the facility that isolates the instrument from ground and pumping vibration. A 320 mm diameter newtonian collimator (F/8.8) located in an additional vacuum chamber, also equipped with an isolated optical bench, is used for optical measurements. The collimator focal plane is composed by a target illuminated by a 150 W Xenon source, out of the vacuum chamber. The target is a 20 mm diameter quartz plate with a chromium coating pattern defining a 20 arcmin diameter angular pattern at the instrument input.

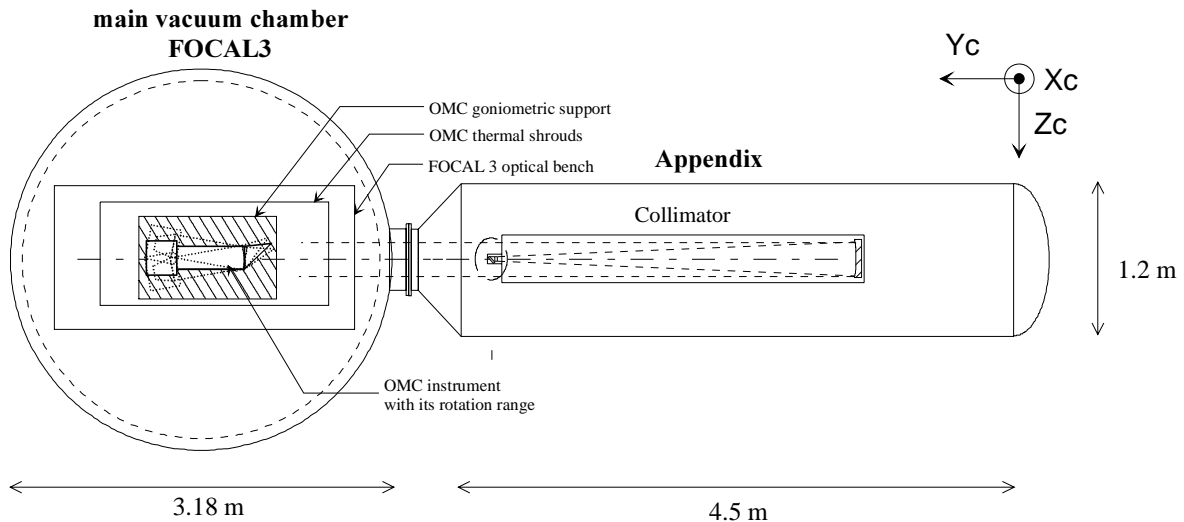


**Figure 9:** FOCAL 3 test set-up

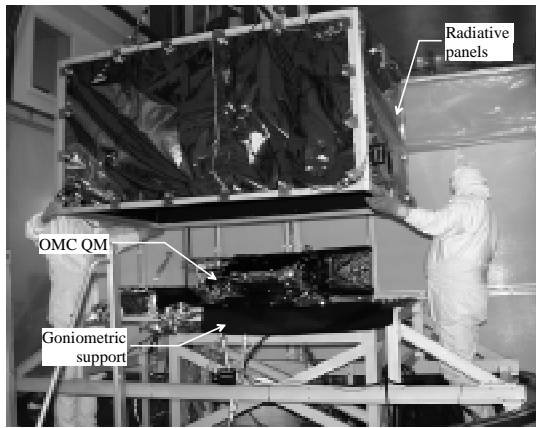


**Figure 10:** Thermal balance test preparation

#### 4.2. Collimator pattern

The collimator pattern was designed such as it allows measuring the Modulation Transfer Function (MTF) using both the Contrast Transfer Function (CTF) and the Line Spread Function (LSF) analysis (figure 11). The CTF is measured by means of two bar pattern with frequencies of  $2/3$  of the Nyquist frequency (24.42 c/mm) and twice the Nyquist frequency (73.26 c/mm). The use of the Coltmann function [4] allows computing the real MTF at  $2/3$  of the Nyquist frequency. The 3.6 arcsec rotation resolution of the goniometric support permits a sub pixel resolution of the CTF measurement. For the LSF, the resolution of the goniometric support is not sufficient and the sub pixel resolution was increased by means of 4 parallel slits separated by  $(n + 1/16)$  pixels where  $n$  is sufficient to avoid neighbourhood effects ( $n \sim 6$  pixels). That pushed the LSF resolution up to  $1/16$  pixel, 1.06 arcsec. This artifice is very insensitive to a non-uniform focal plane illumination as a non-uniformity induces a perturbation whose the frequency is higher than the Nyquist frequency.

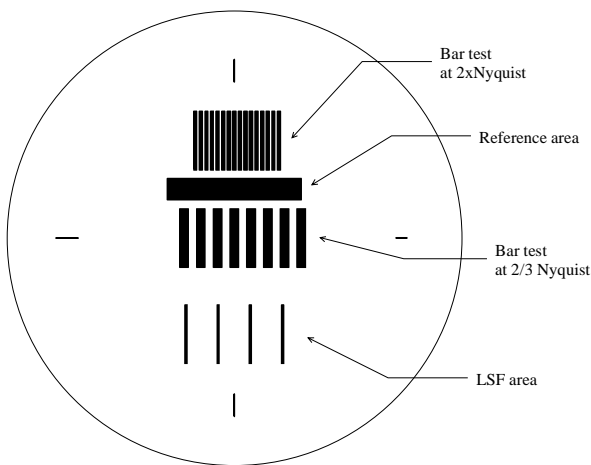


**Figure 11:** Negative view of the target pattern

#### 4.3. Thermal environment

The thermal environment of the thermal balance test is summarised in figure 12. Functional and optical tests were performed at each thermal configuration. Straylight measurements were limited to the nominal case.

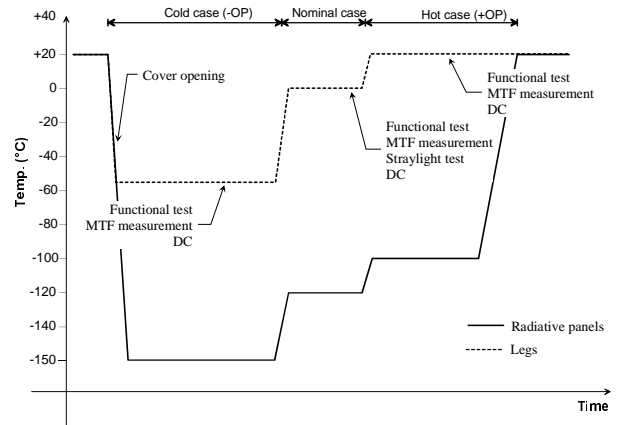


**Figure 12:** thermal environment of the thermal balance test

The thermal environment of the thermal vacuum test is summarised in figure 13: one cycle in the non-operational temperature range followed by 7 cycles in the operational temperature range. Functional and optical check were performed at the beginning and at the end of the operational cycles.

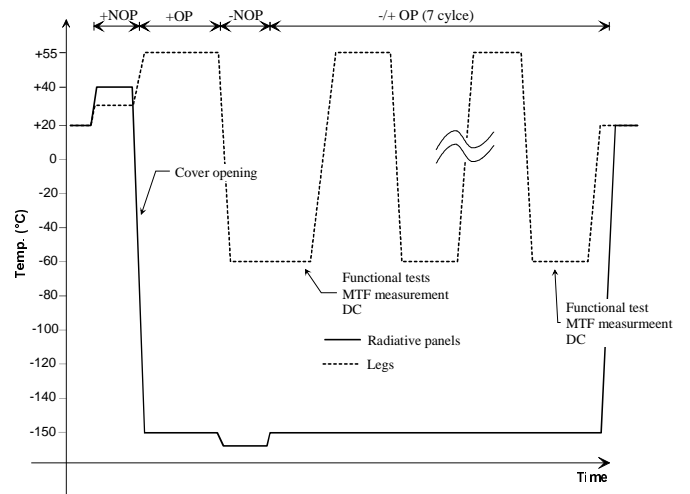


**Figure 13:** thermal environment of the thermal vacuum test

#### 4.4. Lesson learned and FM improvement

The optical performances of the OMC optical system in each thermal configuration are nominal and better than specifications. Nevertheless, two discrepancies



appeared during the MTF measurement and the straylight test.

The first discrepancy is shown in figure 14: a ghost image is presents when a field of view acquisition is performed.

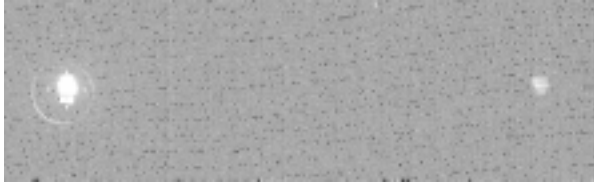


**Figure 14:** Image acquisition in nominal temperature for a 2 arcdeg field of view with the original pattern on the left and the ghost pattern on the right.

The ghost image is perfectly focused and symmetrical with respect to the OMC optical axis. These ghost spots are produced by internal reflections between CCD and filters, mainly the first optical surface, uncoated for radiation purposes. The initial design had underestimated such high reflectivity of the CCD surface. The ghost image was not acceptable for science performances and it was decided to rework the filter assembly housing to put the filter at some angle in order to reject the ghost out of the CCD image area (see figure 15). The tilt angle of the filters is optimum for 4 arcdeg. This modification was implemented for the FM while the QM, used as spare flight model, will be upgraded at the end of the QM campaign.

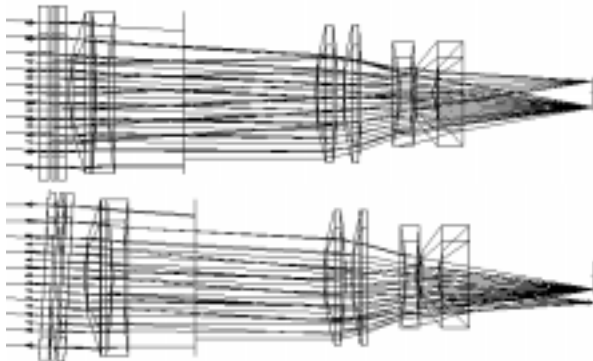


**Figure 15:** ghost spot on the CCD in the untilted QM configuration and ghost spot out of the CCD in the corrected FM configuration

The second discrepancy appeared during the straylight measurements. Figure 16 shows a typical image acquired out of the nominal field of view with a very long exposure to enhance the straylight artefacts. As no direct source was in the field of observation, the image presents several straylight effects: bright spot at the border, blurred disks and crescent.



**Figure 16:** image for a 3 arcdeg field of view

The bright spot at the border appears only for source close of the nominal field of view. It is produced by a grazing reflection on the mask edge above the CCD. This mask protects the electronics from cosmic rays. This effect is unavoidable but has to be limited by a sharper mask edge design.

The blurred disks are originated from internal reflections onto the lens surfaces. They are very faint and common in lens system and can be neglected in this case. The crescent spot origin is more particular: the rear lens bevel produces a direct spot in a crescent shape as shown in figure 17. The simulation correlates the crescent shape and size. To correct this source of straylight, the last spacer has been modified in order to mask the bevel of the last optical surface.

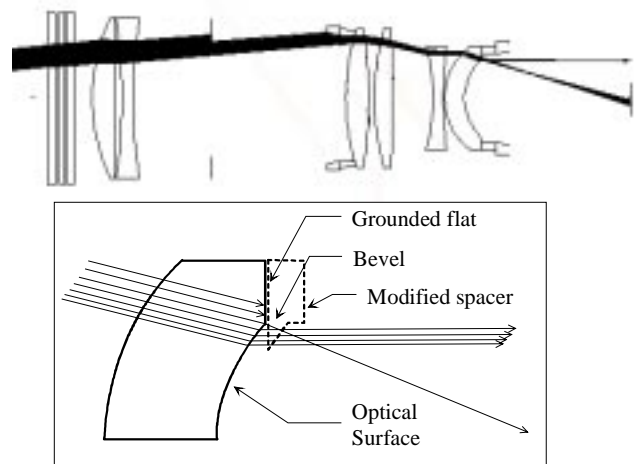


**Figure 17:** Raytracing showing the origin of the crescent straylight and the magnification of the bevel.

## 5. STRAYLIGHT TEST

The test performed on the camera unit QM verified the straylight performances up to  $\pm 10$  arcdeg field of view, inside the unobstructed field of view (UFOV).

In this field, the straylight rejection is obtained mainly by the optical system and the focal plane assembly. In order to verify the main baffle rejection performance outside the UFOV, a specific test was performed on the CSL's FM sub-elements: the optical system, the main baffle and the cover system. The optical system and the cover system are mounted onto the main baffle while the Focal Plane Assembly (FPA) is substituted by a dummy FPA with an identical black cavity shape. A bialkali photocathode photomultiplier was used instead of the CCD detector (figure 18).

The straylight test consisted in comparing the light flux reaching the detector between an on-axis and an off-axis (outside  $\pm 10$  arcdeg field of view) incoming collimated light beam. Neutral density filters in the focal plane were used to avoid detector saturation. The test was performed in ambient condition at 20°C. The collimated beam was produced by 2 m focal length off-axis collimator specially developed for straylight measurements. It is illuminated by an Oriel Photomax lamp equipped with a 150 W Xe lamp. The collimator is set on a movable support at the end of a 2.5 m arm turning around the main baffle entrance. Two 500 mm diameter movable light traps allowed to reduce the environmental straylight: one located in front of the instrument to cover its field of view, the second located in the collimated beam, behind the instrument. The rejection of the light trap is designed to  $10^5$ . The test room is blackened and all electronics are put outside. The 10000 class 10000 cleanliness of the test room is sufficient for the straylight test but, in order to keep the cleanliness of the main baffle and the optical system, the main baffle was purged with dry air through the venting hole.



**Figure 18:** Dummy FPA with the PM photocathode in the focal plane.

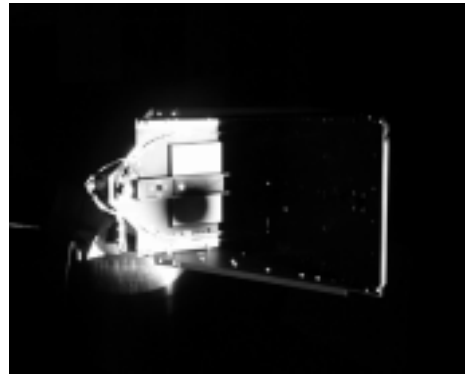


**Figure 19:** Cover system illuminated by the collimator at +20 arcdeg towards the forebaffle (door closed).

Figure 20 shows the measured attenuation at various fields of view. Inside the UFOV ( $\pm 10$  arcdeg field of view), the rejection increases with the field of view, mainly due to the FPA and the optical system. Outside the UFOV, only the main baffle design is efficient.

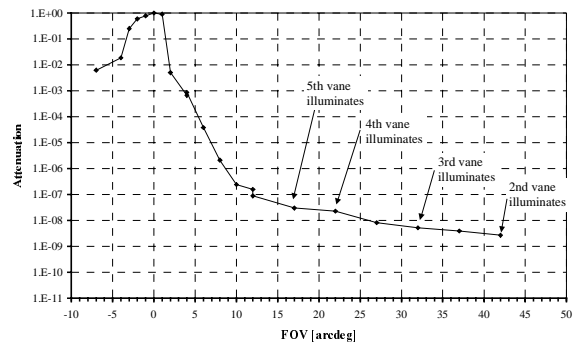


**Figure 20:** Baffle attenuation measured at various fields of view

## 6. FM SUB-SYSTEM ACCEPTANCE

The FM sub-systems manufactured under CSL's responsibility were tested with acceptance levels identical to QM sub-system. For the optical system, a specific test was performed to verify the rejection of ghost images out of the CCD area.

### 6.1. Cover system

The cover system FM was submitted to identical acceptance tests as for the QM. All tests were successfully and no damage was observed during the environmental tests. Functional tests of the door opening were successful.

### 1.6. Optical system

The optical system FM with tilted filters demonstrated improved optical performances with respect to the QM mainly due to improved lens quality. Table 9 summarises the MTF performances

at the Nyquist frequency. In all cases, the performances are higher than the specification (70%).

Field of view [arcdeg]	MTF (38.5 c/mm)
0°	78 – 72 %
1°	74 – 70 %
2°	72 – 70 %
2.5°	72 – 70 %
-1°	76 – 74 %
-2°	75 – 72 %
-2.5°	76 – 73 %

**Table 9:** Maximum and minimum MTF at the Nyquist frequency

Vibration tests and thermal vacuum tests were successful and no damage was observed. Table 10 presents the WFE measurements (at  $\lambda = 633$  nm) performed between each environmental test: no significative variation was observed.

	Wavefront PV [wave]	Wavefront RMS [wave]
Reference	0.727	0.108
Post vibration	0.598	0.096
Post thermal vacuum	0.680	0.110

**Table 10:** FM WFE measurement results

A specific test was performed to verify the location of the ghost image due to internal reflection between the CCD and the filters. To increase the ghost intensity, the CCD was replaced by a simple flat mirror as shown in Figure 21. In all cases, the ghost image is largely outside the CCD area.

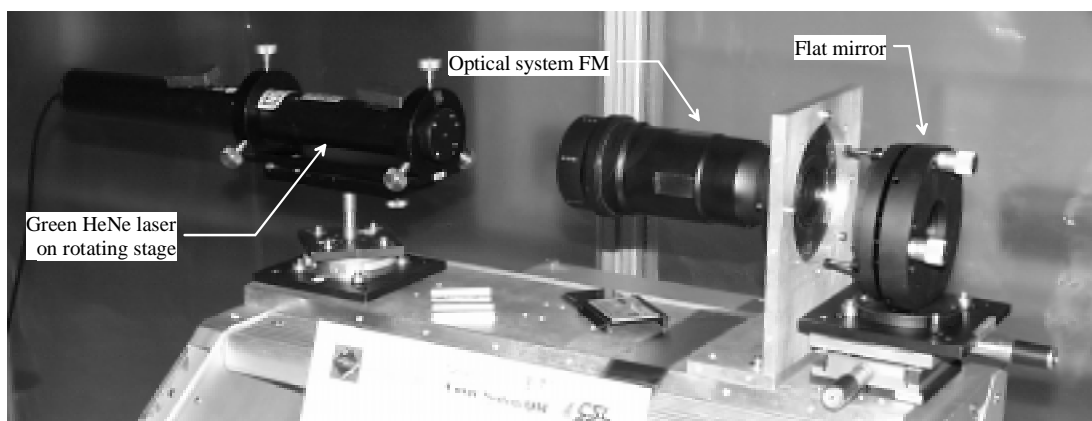


**Figure 21:** Set-up of the ghost test

## 7. CONCLUSIONS

The OMC program has been successfully developed with intensive testing at component level. However, specific improvement of the hardware could only be defined after the first end-to-end verification of the complete QM instrument. This outline the need to start tests on the complete model as early as possible in the development program of the instrument. The measured performances of the QM reached the initial specifications although part of it could be relaxed once the launcher and orbit were confirmed.

## 8. ACKNOWLEDGMENT

The Belgian part of the OMC program is developed with support from OSTC. This work is performed in the frame of the OMC international consortium.

## 9. REFERENCES

- <sup>1</sup> E. Mazy, J.M. Defise, J.Y. Plesseria, "Optical Design of the INTEGRAL Optical Monitoring Camera", SPIE 3426, 1998
- <sup>2</sup> E. Mazy, J.M. Defise, J.Y. Plesseria, "INTEGRAL Optical Monitoring Camera Stray-Light Design", SPIE 3426, 1998
- <sup>3</sup> E. Mazy, J.Y. Plesseria, E. Renotte, P. Rochus, "Acceptance Tests of the INTEGRAL Optical Monitoring Camera Sub-System", SPIE 3785, 1999
- <sup>4</sup> R.L. Lucke, "Deriving the Coltman Correction for transforming the bar transfert function to the optical transfert function", Applied Optics, Vol 37, n° 31, 1998